

# Exergy and economic analysis of a micro-cogeneration system coupled with a biomass gasifier

B. Morrone<sup>a,\*</sup>, P. Bracciano<sup>a</sup>, D. Cirillo<sup>b</sup>, M. La Villetta<sup>b</sup>, C. Caputo<sup>b</sup>

<sup>a</sup> Dip Ingegneria – Università della Campania “L. Vanvitelli”, Aversa, (CE), 81031, Italy

<sup>b</sup> Costruzioni Motori Diesel CMD SpA, San Nicola La Strada, (CE), 81020, Italy

## ARTICLE INFO

### Keywords:

Micro cogeneration  
Gasification  
Biomass  
Internal combustion engine  
Exergy analysis

## ABSTRACT

Biomass serves as a solution to the energy crisis and aids in lowering greenhouse gas emissions. Residual biomass, a significant portion of total biomass, is abundant globally and can be utilised to produce energy, biofuels and biomaterials, without encroaching upon the food sector. In this paper, an energy, exergy, economic and environmental analysis of a micro-cogeneration system coupled with a wood biomass downdraft gasifier is carried out. The gasification produces syngas, mainly CO, H<sub>2</sub> and CH<sub>4</sub>, used as fuel for internal combustion engines with cogeneration aims. Two types of wood biomass are tested and compared: briquettes from pruning and pine wood chips. The experimental investigation is carried out by instrumenting both the biomass gasifier and the internal combustion engine. The nominal electric and thermal power are 20 kW<sub>e</sub> and 40 kW<sub>th</sub> respectively. The results demonstrate the full feasibility of the energy valorisation of residual organic materials. In fact, the whole plant shows energy efficiencies of 47 % and 32 %, and exergy efficiencies of 21 % and 14 %, for the two investigated feedstocks. The economic analysis shows that the main indicators of the micro-cogeneration plant are positive with Profitability Index between 13 %, worst scenario, and 193 %, for the most favorable scenario. The GHG emissions display reductions equal to approximately 60–95 t/y, giving biomasses a decisive role in the challenge of decarbonization and reduction of GHG emissions.

Symbol	Description	Unit of measure
<i>c</i>	Specific heat	kJ/(kg K)
<i>C</i>	Cost	€
DPB	Discounted Payback time	y
<i>EX</i>	Exergy flow rate	kW
<i>ex</i>	Specific exergy	kJ/kg
<i>h</i>	Enthalpy	kJ/kg
<i>H<sub>eq</sub></i>	Equivalent hours per Year	h/y
HHV	Higher Heating Value	kJ/kg
LHV	Lower Heating Value	kJ/kg
<i>M</i>	Moisture	%
<i>m</i>	Mass Flow Rate	kg/s
mCHP	Micro Combined Heat and Power system	–
NPV	Net Present Value	€
<i>P</i>	Power	kW
PI	Profitability Index	%
<i>P<sub>bm</sub></i>	Specific price of biomass	€/ton
<i>P<sub>ee</sub></i>	Specific price of electricity	€/kWh
<i>P<sub>CNG</sub></i>	Specific price of Natural Gas	€/Scm
<i>Q</i>	Thermal Power	kW
SPB	Simple Payback time	y

(continued on next column)

(continued)

Symbol	Description	Unit of measure
<i>T</i>	Temperature	K
<i>w</i>	Water mass Fraction	kg/kg
<i>W<sub>el</sub></i>	Electric Power	kW
<i>x</i>	Molar fraction	–
<i>γ</i>	Cogeneration ratio <i>E<sub>el</sub>/E<sub>th</sub></i>	–
WACC	Weighted average capital cost	%
<i>δ<sub>i</sub></i>	Efficiency defect	–
<i>η</i>	First law Efficiency	–
<i>η<sub>ex</sub></i>	Exergy Efficiency	–
<i>λ</i>	Air-fuel ratio	kg <sub>a</sub> /kg <sub>fuel</sub>
<i>τ</i>	Carnot factor	–
<i>φ</i>	Ratio exergy to LHV	–

### Abbreviations

CGE Cold Gas Efficiency  
HX Heat Exchanger  
PHX Plate Heat Exchanger  
STHX Shell Tube Heat Exchanger

### Subscripts

*a* Air

(continued on next page)

\* Corresponding author.

E-mail address: [biagio.morrone@unicampania.it](mailto:biagio.morrone@unicampania.it) (B. Morrone).

(continued)

Symbol	Description	Unit of measure
<i>ar</i>	As received	
<i>bm</i>	Biomass	
<i>Ch</i>	chemical	
<i>daf</i>	Dry ash free	
<i>db</i>	Dry basis	
<i>des</i>	Destroyed exergy	
<i>dry</i>	Dry value of $\phi$	
<i>el</i>	Electrical	
<i>exh</i>	Exhaust gases	
<i>g</i>	gasifier	
<i>ICE</i>	Internal Combustion Engine	
<i>Moist</i>	Air moisture	
<i>ph</i>	physical	
<i>rxn</i>	Reaction value	
<i>Syn</i>	Syngas	
<i>Th</i>	Thermal	

## 1. Introduction

The energy sector accounts for more than 30 % of greenhouse gas (GHG) emissions today in the World [1], with an increment of more than 80 % considering 1990 as a reference year. Reducing global carbon dioxide (CO<sub>2</sub>) emissions to net zero by 2050 is consistent with the efforts to limit the long-term increase in average global temperatures to 1.5 °C [2] and it is the key to tackling humankind's greatest challenge. This requires a complete transformation of production, transport, and energy consumption. The growing political consensus on reaching net zero is cause for considerable optimism about the progress the world can make, but the changes required to reach net-zero emissions globally by 2050 are poorly understood [3].

In addition to this world challenge, the Ukraine-Russia war dramatically increased natural gas prices, especially in Europe. The price at the Amsterdam Market jumped from about 23 €/MWh as of July 2021 to more than 340 €/MWh as of August 2022, more than ten times the pre-crisis price.

The increase in energy prices had tremendous outcomes for industrial and domestic consumers. Many industries, mainly those using tons of natural gas, either increased prices of the final products, creating the spiral of modern inflation or cutting job places by stopping production. Inflation with values of about 10 % in most European countries [4] as of December 2022, on year basis, reduced to 6.1 % on May 2023. Considering only the Energy inflation rate, it spanned from 39 % in May 2022 to -1.8 % as of May 2023 on a yearly basis. This situation forced people to reduce buying of goods, creating a very difficult economic situation in many European countries.

Energy, economic and social issues would require an immediate response from the political and stakeholder' sides. Many possible solutions are sought that can also cope with the climate crisis, thus resulting from what is known as "Green Transition" [5].

Biomass serves as a solution to the energy crisis and aids in lowering greenhouse gas emissions. Residual biomass, a significant portion of total biomass, is abundant globally and can be utilised efficiently to produce not only energy but also biofuels, and biomaterials without encroaching upon the food sector. However, the diverse chemical and physical properties of biomass necessitate distinct thermochemical, biochemical, or physical-chemical conversion pathways to yield energy or extract biofuels and biomaterials directly [6,7].

Cogeneration, for short CHP (Combined Heat and Power), is the simultaneous production of different forms of useful energy using only one single energy source [8–12]. The principal useful forms of energy produced are electrical and thermal energies. A recent paper by Jie et al. [13] performed an economy, energy, and environmental optimization of a biomass gasification combined cooling, heating, and power system integrated with a ground source heat pump. The results are reported in terms of cost, GHG emission, and cumulative savings, showing a ranking of the different configurations when the electric or thermal loads are

followed.

The request for local energy production and social policy targets in the last years has drawn attention on the small-scale energy conversion systems, mainly in the range of 20 kW to 1 MW, together with the reduction of greenhouse gas emissions [8]. In addition, several examples of biomass-fired CHP plants based on the organic Rankine cycle (ORC) with a size in the range of 400–1500 kW exist and they are commercially available with an electric efficiency of about 20 % [14].

The new challenges faced in the green transition would require more decentralized and flexible power systems, and for this reason, the development and operation of biomass-powered CHP units is of great importance, mainly micro-scale CHP (mCHP) system. An interesting and extensive review of the available solutions for mCHP systems is reported in Ref. [8]. The authors point out that internal combustion engine (ICE) technology seems to be the most mature and economically viable solution. CHP systems based on biomass gasifiers coupled with ICEs have been developed at a commercial scale. Their flexibility and efficiency in biomass conversion is a major advantage [9,15] further enhanced by the reliability of the operation of ICEs. In Ref. [16] the authors reported a list of m-CHP systems integrated with different gasifier technologies located in many places around the globe. The electric efficiency ranges from a poor 5 % to a massive 30 %, whereas the global efficiency equals 30–95 %. They also listed the type of gasifier employed: Downdraft (DD), Updraft (UD), Fluidized Bed Gasifier (FBG) and Pressurized Fluidized Bed Gasifier (PFBG), the last one used mainly for plants larger than 2 MWe.

Biomass gasification has been largely developed in the past years, and nowadays, it can be considered quite attractive as it works with different energy sources and usually causes less environmental pollution than the conventional combustion process. The gasification process primarily transforms solid or sufficiently dry feedstock into gaseous products through incomplete oxidation at high temperatures, typically ranging between 800 and 1000 °C, with oxygen supplied below stoichiometric levels. The equivalence ratio (ER), indicating the ratio of supplied oxidant to that needed for complete combustion, typically falls within the range of 0.20–0.45 and significantly influences the resulting syngas composition. The outcome of gasification reactions yields a mixture of gaseous compounds, including carbon dioxide, water, carbon monoxide, hydrogen, gaseous hydrocarbons, along with minor quantities of solid char, ash, and condensable compounds like tars and oils. Steam, air or oxygen can be supplied to the gasification process as oxidizing agents. The produced gas is easier to use as a fuel than the original feedstock [12,17].

Gasification systems for CHP systems are becoming more appealing both from technical and economic point of views, especially when residual biomass is largely available and easily collectable. Among them, solid wood residues represent an important feedstock for several reasons; one is their large availability, another is related to the conversion of hardwood residues to woodchips offering an increment of their energy density and thus economic revenue. This could allow the national energy grid systems to be supported by independent small to large CHP systems, relying less on energy sources imported from abroad. In Europe, oil and petroleum products (including crude oil), account for 63 % of energy imports into the EU, followed by natural gas (26 %) and solid fossil fuels (7 %) [18].

The results of a co-gasification of lignite and waste wood in a downdraft gasifier were shown in Ref. [19]. The authors stated that there are some advantages in co-gasifying woody biomass and coal, as the addition of waste wood can adjust the ash content of the mixtures. In addition, waste wood is easily available as agricultural or forest residue, and its collection in remote regions can be cheap.

Six different biomasses were tested in a lab-scale prototype in Puglia et al. [20] evaluating the elemental and ash analyses. The results showed that the tested agro-industrial residues performed acceptably in terms of efficiency, and the produced char had a carbon content of over 70 % as a by-product.

The review presented by Mishra et al. [21] gives an interesting

overview of different types of biomass utilised in hydrogen production by using gasification and pyrolysis routes for biomass transformation into energy. The syngas obtained via biomass gasification significantly affects hydrogen production. The authors assert that algal biomass is a valuable material for the third generation of biofuel feedstock because of its benefits. The perspectives on enhancing hydrogen production are also presented in the paper.

Havilah et al. [22] reviewed the gasification-based bioenergy production. They claim that the process can replace fossil fuels and reduce CO<sub>2</sub> emissions. They state that there is still opportunity for improvement in terms of high-quality syngas generation (high H<sub>2</sub>/CO ratio) and reduced tar formation, which considerably impacts syngas quality. Their review found that downdraft gasifiers show significant potential for producing high-quality syngas with lower tar concentrations.

Hydrogen (H<sub>2</sub>) is emerging as a pristine energy alternative, derived from diverse sources via advanced processes. The authors in Ref. [23] scrutinised state-of-the-art gasification technologies and catalysts for H<sub>2</sub>-rich syngas production, including innovative methods like solar and microwave gasification.

MSW-to-multi-generation energy systems via gasification offer eco-friendly waste disposal, clean energy generation, reduced reliance on fossil fuels, and lower emissions. In Ref. [24] a novel system combining a fluidised bed gasifier, SOFC, and heat recovery is presented. The authors highlight enhanced efficiencies and reduced emissions with increased steam-to-MSW ratio and utilisation factor, along with optimized current density and SOFC temperature. They claim that the approach presents a sustainable solution for waste management while meeting clean energy demands.

A new method for continuous tar monitoring in hot syngas from biomass gasification is presented. It involves extracting a small syngas sample and determining tar combustion oxygen demand using synthetic air. Laboratory tests show promising sensitivity and stability. However, field tests on woodchip-fueled gasifier syngas revealed challenges due to continuous variations in composition, thus impacting the accuracy of the measurements [25].

A thorough understanding of the physicochemical properties of lignocellulosic biomass and the analytical methods used for characterisation is crucial for designing and operating biomass conversion facilities. In Ref. [26] the authors aimed to present fundamental information of the physicochemical properties of lignocellulosic biomass and characterisation techniques relevant to biomass conversion and biofuel applications. The physicochemical properties of lignocellulosic biomass serve as essential reference data for designing and implementing these processes. The authors conducted a material balance analysis to develop an empirical stoichiometric equation describing wood chip gasification in a downdraft gasifier. This equation is derived from experimental data overall and elemental material balances, with adjustments made to ensure the material balance closure.

In [27] the authors examined the material balance analysis to establish an empirical stoichiometric equation for wood chip gasification in a downdraft gasifier. This formulation is based on overall elemental material balances obtained from experimental data. To achieve material balance closure, the data were two-tier adjusted.

Pretreatment processes as drying, grinding and sieving of feedstocks are often required when using biomass feedstock. The conversion process includes feeding, conversion, separation of intermediate products, collection and upgrading of products. The properties of biomass are essential data of reference for the design and implementation of these processes. In Refs. [28,29] the authors developed methods for estimating the HHV of solid, liquid, and gaseous fuels, which is essential in assessing the potential of biomass and affects the efficiency indices of the process.

As already highlighted, decentralized energy production plants can represent a solution, together with the use of renewable energies, such as biomass, to tackle both the GHG and economic issues. Thus, a micro cogeneration power (mCHP) system syngas fed from biomass

gasification represents a perfect device for facing these issues. Some commercial examples of mCHP systems coupled with a gasifier are available on the market. One such system is the HKA35 from Re<sup>2</sup> (Germany), which has a nominal electrical power of 35 kW<sub>e</sub> and operates with a wood chips consumption of 31.5 kg/h. Another notable example is the CHP Eco 50 HG from Burkhardt, offering a nominal electrical power of 50 kW<sub>e</sub> and thermal output of 85 kW<sub>th</sub>, with a power-to-heat ratio of 0.59. An Italian company, Reset-Energy, offers Power-Skid systems with capacities ranging from 50 to 200 kW<sub>e</sub>, a nominal power-to-heat ratio of 0.68, and biomass consumption between 60 and 240 kg/h. To the best of the authors' knowledge, no other compact systems integrating a CHP unit and a gasifier are currently available on the market with a nominal power output below 100 kW<sub>e</sub>. This suggests a potential gap in the market for smaller-scale, integrated solutions that could meet the needs of residential or small industrial applications.

This paper presents an analysis of a micro-cogeneration system that integrates a biomass downdraft gasifier, focusing on energy, exergy, economic, and environmental aspects. The experimental investigation involves comprehensive instrumentation of both the biomass gasifier and the internal combustion engine powered by syngas. The system has a nominal power of 20 kW<sub>e</sub> and a thermal output of 40 kW<sub>th</sub>, resulting in a power-to-heat ratio of 0.5.

The proposed micro-cogeneration system combines a downdraft gasifier with an internal combustion engine (ICE) specifically optimized for syngas operation, offering superior energy conversion efficiency and cost-effectiveness compared to conventional systems. Its compact and portable design allows for effortless transportation using a medium-sized truck, without the need for specialized equipment.

Two different types of wood biomass are tested and compared to demonstrate the largely feasible and the decisive role for final users in the reduction of GHG emissions thanks to the large availability of residual biomass. In the experimental tests, the Cold Gas Efficiency (CGE) of pine wood chips achieved 82.8 %, demonstrating superior performance. At the same time, the system's flexibility allows it to utilize diverse biomass feedstocks, including low-cost pruning briquettes. The system's ability to process diverse biomass types allows users to optimize operational expenses based on feedstock availability and cost. Pruning briquettes, often considered waste from agricultural and green maintenance activities, represent a highly economical feedstock option. They are typically either freely available or sold at a minimal cost, thereby reducing the dependency on purchased wood chips or other high-cost alternatives. Despite their slightly lower energy performance compared to pine wood chips, pruning briquettes offer a substantial cost advantage for users with access to these residual biomasses.

The economic analysis highlights significant cost savings compared to traditional energy systems. Scenarios involving free or low-cost biomass yield exceptionally high profitability indices (PI) of up to 193 % and discounted payback times (DPB) as short as 3.4 years, even when accounting for system maintenance and operational costs. The ability to use multiple feedstocks ensures steady operational costs regardless of market fluctuations in feedstock or energy prices, enhancing long-term economic resilience.

The CO<sub>2eq</sub> savings stress the environmental benefits of these systems. Using pine wood chips results in annual savings of 66.19–94.55 tons. Briquettes provide savings of 60.28 tons and 86.12 tons under the same conditions. These results underscore the significant potential of biomass CHP systems in reducing emissions, with pine wood chips offering a clear advantage in both efficiency and environmental impact.

## 2. Analysis and Modelling

The biomass is processed by an ECO20x micro-cogeneration plant with a nominal power of 20 kW electric and 40 kW thermal [16,30], designed and built by CMD. The system is comprised of a gasifier and an internal combustion engine. The plant is designed to process G30 (30 mm) size biomass with a moisture degree of around 20 %. The biomass

**Table 1**

Main data of the internal combustion engine used for CHP.

Cylinders	6
Type of engine	Naturally aspirated
Ignition	Spark ignition
Cooling system	Water
Displacement	4.294 L
Compression ratio	9.4:1
Bore diameter	101.6 mm
Stroke	88.0 mm

undergoes a thermochemical conversion process inside the gasifier. This produces syngas, once suitably filtered and cleaned of impurities by the syngas cleaning system, is used as fuel in the engine, which produces electricity. On the other hand, the thermal energy is recovered by two heat exchangers from the engine coolant and exhaust combustion gases.

The engine is a PSI (4X) 4.3L 6-cylinder naturally aspirated, liquid-cooled and suitably adapted for syngas operation. Engine details are listed in Table 1. The alternator is brushless with 2 pole pairs, with a phase-to-phase output voltage of 400 V at 50 Hz.

The analysis considers two different ligno-cellulosic biomasses: pine wood chips and briquettes from pruning. The biomasses undergo several pre-processing steps, the most important being drying followed by grinding and making the briquettes for inserting them into the gasifier's hopper.

Fig. 1 shows the whole plant with all its devices and equipment. When analyzing the plant, simplifications are required for writing down the energy and exergy balances.

$$\begin{cases} m_{bm}LHV_{bm} + m_{a,g}c_{p,a}(T_a - T_{STD}) = m_{syn}(LHV_{syn} + c_{p,syn}(T_{c1} - T_{STD})) + m_{char}LHV_{char} \\ + m_{ash}c_{p,ash}(T_{c1} - T_{amb}) + m_{moist}\Delta h_{moist} + Q_{loss} \\ m_{a,g}(ex_{a,g}^{ch} + ex_{a,g}^{ph}) + m_{bm}(ex_{bm}^{ch} + ex_{bm}^{ph}) = m_{syn}(ex_{syn}^{ch} + ex_{syn}^{ph}) + Q_{loss}\tau_g + EX_{des,CV1} \end{cases} \quad (3)$$

The employed control volumes, streams of matter and energy fluxes are reported in Fig. 2. The streams entering and exiting the control volumes (C.V.) are represented by dashed lines with different colours, whereas electrical power is with a thick arrow. The whole system is enclosed in C.V.ECO, whereas C.V.1 comprises the gasifier system with the filtering section, required to clean the exiting syngas, and C.V.2 consists of the internal combustion engine (ICE) and heat exchangers (HXs) for heat recovery. The HX system is composed of the radiator of the ICE, a plate HX (PHX) heat exchanger and a shell and tube HX (STHX) heat exchanger, which recovers the thermal energy of the ex-

$$\begin{cases} m_{syn}(LHV_{syn}) + m_{a,ICE}h_{a,ICE} = W_{el} + m_{exh}c_{p,exh}(T_{exh,in} - T_{amb}) + Q_{jacket} + Q_{eng,loss} \\ m_{a,ICE}(ex_{a,ICE}^{ch} + ex_{a,ICE}^{ph}) + m_{syn}(ex_{syn}^{ch} + ex_{syn}^{ph}) + m_w(ex_w^{ch} + ex_w^{ph})_{IN} = \\ m_{syn}(ex_{syn}^{ch} + ex_{syn}^{ph}) + m_w(ex_w^{ch} + ex_w^{ph})_{OUT} + Q_{eng,loss}\tau_{eng} + EX_{des,CV2} \end{cases} \quad (4)$$

hausts of the ICE. The HX radiator can be bypassed by the cooling fluid of the ICE when its temperature at the outlet of the engine is below a predefined threshold.

Table 1 displays the main parameters of ICE used for CHP purposes and fueled by syngas from the gasifier.

## 2.1. Energy and exergy analysis

The mass balances applied to the C.V.2 and to the ICE are the following:

$$\begin{cases} m_{a,g} + m_{bm} = m_{syn} + m_{res} \\ m_{a,g}w_{N_2}^{a,g} = m_{syn}w_{N_2}^{syn} \\ m_{a,ICE} + m_{syn} = m_{exh} \end{cases} \quad (1)$$

The known mass flow rates are  $m_{bm}$ , obtained by measuring the biomass loaded in the hopper and the time interval,  $m_{a,g}$  the air entering the gasifier,  $m_{a,ICE}$  and  $m_{exh}$  the mass flow rates of air entering and the exhausts from the ICE, measured using a pitot tube, respectively.

The air mass flow rate in the gasifier is obtained by using a partial balance of nitrogen on the gasifier, as reported in Eq. (1), where  $w_{N_2}^{a,g}$  and  $w_{N_2}^{syn}$  represent the mass fraction of nitrogen in the air entering the gasifier and in the syngas leaving the gasifier, respectively. By measuring the value of air sucked by the engine, it is possible to obtain the unknown values of the mass flow rates.

The residual mass flow rate  $m_{res}$  is given by the sum of all the products from the filtering system, i.e.:

$$m_{res} = m_{char} + m_{moist} + m_{ash} \quad (2)$$

The mass flow rate of char  $m_{char}$  is evaluated as a percent fraction of the inlet biomass [27],  $m_{moist}$  the moisture content and the ash flow rate is obtained by difference from Eq. (2).

The energy and exergy balances for the gasifier, using the C.V.1, are written as in Eq. (3):

with  $LHV$  the lower heating value of the substances ( $bm$ ,  $syn$  and  $char$ ) and  $T_{c1}$  the average temperature inside the gasifier, obtained from measurements,  $Q_{loss}$  the heat losses from the gasifier body to the environment and  $\tau_g$  is the Carnot factor, in this case equal to zero. Assembling the chemical exergies of the streams of the matter, the chemical exergy of the reaction is obtained.

For the internal combustion engine, the energy and exergy balances are reported in Eq. (4):

The process performance evaluation is discussed using the following efficiency parameters:

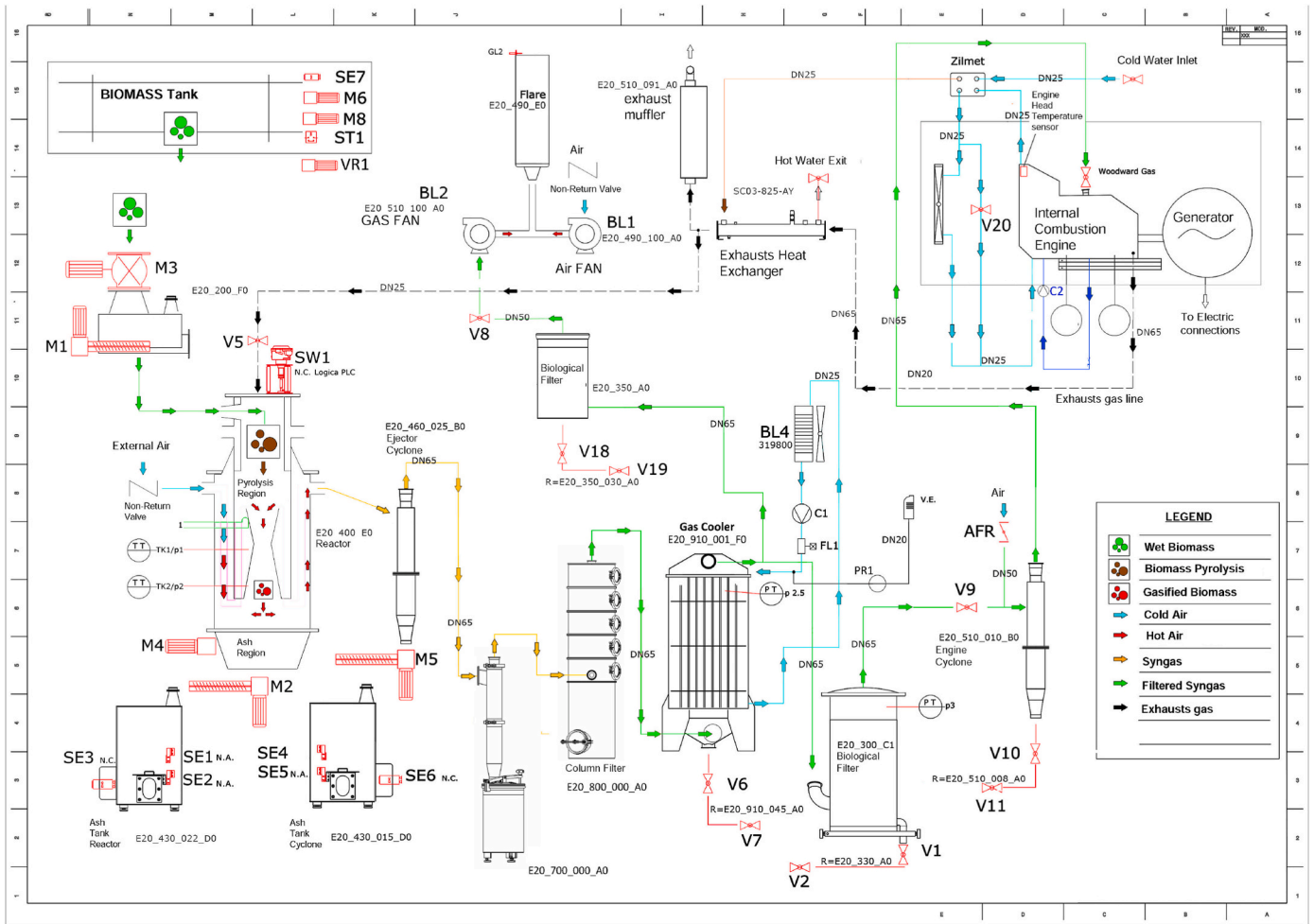


Fig. 1. Sketch of the analyzed plant.

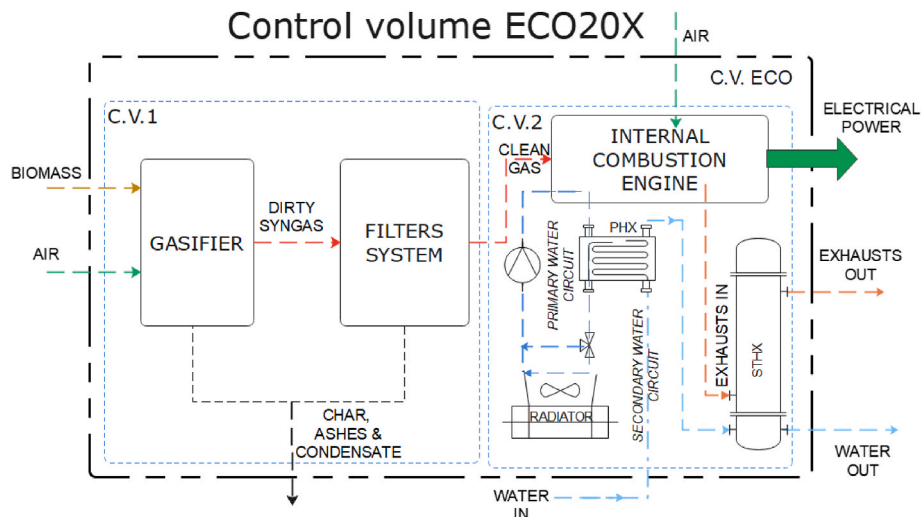


Fig. 2. Control volumes for the Energy and Exergy analyses.

$$CGE = \frac{P_{syn}}{P_{bm}};$$

$$\eta_{el,ICE} = \frac{W_{el}}{P_{syn}}; \eta_{th,ICE} = \frac{Q_{PHX} + Q_{STHX}}{P_{syn}} \quad (5)$$

$$\eta_{gl,ICE} = \eta_{el,ICE} + \eta_{th,ICE}$$

$$\eta_{gl,pl} = CGE \times \eta_{gl,ICE}$$

with CGE the Cold Gas Efficiency, which represents the percentage of the biomass heating value recovered in the gasifier product gas. The energy efficiencies reported in Eq. (5) refer either to the internal combustion engine (ICE) or to the whole plant ( $pl$ ). The exergy efficiencies and defects of efficiencies are reported in Eq. (6):

$$\eta_{ex,gas} = \frac{EX_{syn}^{ch}}{EX_{bm}^{ch}}; \eta_{ex,ICE} = \frac{EX_{el} + (Q_{PHX}\tau_{PHX} + Q_{STHX}\tau_{STHX})}{EX_{syn}^{ch}} \quad (6)$$

$$\delta_i = \frac{EX_{des,i}}{EX_{in,i}} \quad \text{for } i = gas, ICE, STHX, PHX$$

with  $\tau$  being the Carnot factor for each HX and defined as:

$$\tau_i = \left(1 - \frac{T_0}{T_f}\right) \quad (7)$$

with  $T_0$  being the environmental temperature (expressed in K) and  $\bar{T}_f$  the average temperature of each fluid flowing in the HX.

The physical exergy of the streams is calculated, according to Kotas [31], as:

$$ex_{ph} = (h - h_0) - T_0(s - s_0) \quad (8)$$

with the terms with the subscript 0 refer to the environmental conditions (restricted equilibrium), chosen as  $T_0 = 298$  K and  $p_0 = 1$  bar. The chemical exergy assessment depends on the type of substance under consideration. The chemical exergy of the biomass has been related to the LHV by using a correlation equation which considers the elemental composition [31] for solid fuels, when the ratio  $o/c$  is in the range 0.667 and 2.67.

$$\varphi_{dry} = \frac{1.0438 + 0.1882\frac{h}{c} - 0.2509\left(1 + 0.7256\frac{h}{c}\right) + 0.0383\frac{n}{c}}{1 - 0.3035\frac{o}{c}} \quad (9)$$

where  $h, c, n, o$  represent the mass fractions of the corresponding chemical species. The value calculated in Eq. (9) is employed to assess the chemical exergy of the solid fuel:

$$ex_{ch} = [LHV + wh_{fg}] \varphi_{dry} \quad (10)$$

neglecting the sulphur content, which is null for the investigated biomass, and  $w$  being the moisture of the biomass and  $h_{fg}$  the latent heat of evaporation of water.

The computation of chemical exergy of ideal gas mixtures is obtained as:

$$ex_{ch,MIX} = \sum_k x_k ex_{ch,k} + RT_0 \sum_k x_k \ln(x_k) \quad (11)$$

where  $k$  represents each component of the mixture.

## 2.2. Economic analysis

The economic analysis is based on discounted cash flows. The analysis is carried out as a comparison between the proposed micro cogeneration plant and the traditional purchase of electric and thermal energies, obtained using a boiler. The cash flows account for the initial capital investment  $C_0$  (*capex*) and the annual cash flow due to the potential biomass purchase and the annual maintenance costs. Comparing the two situations the over cost is given by the cost of the plant since the

traditional system does not involve any initial (relevant) costs, whereas the annual saving, indicated as  $S_k$ , is given by the difference between the expenditure of the traditional energy cost and that arising from the biomass plant. Defining a time horizon for the lifetime of the plant equal to 15 years, the main economic indices computed are the Net Present Value, NPV:

$$NPV = \sum_{k=1}^N S_k (1 + WACC)^{-k} - C_0 \quad (12)$$

with WACC being the Weighted Average Capital Cost, as defined in Refs. [32,33] and represents the discount rate, balancing the equity and debt cost of money,  $S_k$  the annual cash flow (saving). The discounted payback time is calculated as in Eq. (13):

$$\sum_{k=1}^{DPB} S_k (1 + WACC)^{-k} = C_0 \quad (13)$$

The annual O&M cost of the micro cogeneration plant is given by: the cost of the purchased biomass in case not available to the user site and the cost of annual maintenance of the gasifier, ICE and HXs. Thus, the  $S_k$  is given by:

$$S_k = (C_{Ele} + C_{ET}) - (C_{bm} + C_{mnt}) \quad (14)$$

where  $C_{Ele}$  and  $C_{ET}$  are the cost of purchase of the electric and thermal energy of the traditional system and  $C_{bm}$  the cost of purchase of biomass and  $C_{mnt}$  the cost of mCHP maintenance.

The Payback time, either Simple or Discounted, is calculated as the time necessary to equal the initial investment cost. For the discounted payback it is:

$$C_0 = \sum_{k=1}^{DPB} S_k (1 + WACC)^{-k} \quad (15)$$

The main hypotheses employed for the economic evaluation are the following: the WACC and the yearly saving  $S_k$  are constant throughout the entire lifetime of the project.

## 3. Materials and methods

Several types of bases are commonly used for expressing biomass analysis results. They are “as received basis” (*ar*), “air dried basis” (*adb*), “dry basis” (*db*), and “dry ash free basis” (*daf*) [34]. The *as received* basis shows the results using the total weight of sample as it arrived at the laboratory and prior to any pre-treatment. Dry basis is when biomass is free from moisture neglecting all moistures both external and inherent moistures. Dry ash free basis present data in which the sample is free from both all moistures and ash. This is frequently used in ultimate analysis to show the contents of elements in the organic fractions of the biomass sample.

The calculation of the LHV for the biomass is obtained from the HHV<sub>(dry)</sub> value, based on the elemental composition and using the moisture,  $w$ , and hydrogen mass percentage,  $h$ , in the biomass composition [34], as in:

**Table 2**

Data for energy and exergy balances from experimental tests or calculated.

Quantity	Pine Wood chips	Briquette
Biomass quantity (kg)	102	108
Time interval (h)	3.34	2.47
Biomass flow rate (kg/h)	28.6	38.8
Exhaust flow rate (kg/h)	152	153
$\lambda_{eng}$	1.05	1.025
Electrical Power (kW)	19.95	18.17
Water flow rate primary circuit (kg/s)	0.48	0.50
Water flow rate secondary circuit (kg/s)	0.22	0.20
LHV <sub>bm ar (dry)</sub> (MJ/kg)	12.46 (14.82)	14.22 (15.54)

$$LHV_{(ar)} = HHV_{(dry)}(1 - w) - 2.44(9h + w) \quad (16)$$

The syngas is sampled and analyzed at the exit of the gasifier and the exhausts at the exit of ICE by collecting gases in aluminum tanks using an Agilent 990 micro gas chromatograph, with the main gases previously quantified using standard mixtures of known composition.

The biomass's elemental composition, i.e., the mass fraction of carbon, hydrogen, nitrogen, sulphur and oxygen (the last evaluated by difference), is determined using a LECO CHN-S 628. The measurement method is based on the complete and instantaneous oxidation using pure oxygen (dynamic flash combustion) of the samples with their conversion into gaseous products. Their quantitative estimation is obtained either by non-dispersive IR or thermal conductivity cells.

The proximate analysis provides moisture, volatile matter, fixed carbon, and ash content, while the ultimate analysis gives the fuel composition in terms of its basic elements such as carbon, hydrogen, nitrogen, sulphur, and oxygen (evaluated by difference). In this work, the proximate analysis was performed drying the gross biomass sample in air to 105 °C for 12 h. Then, the dried sample was heated to 950 °C in inert ambient (nitrogen) for 7 min to obtain volatile matter (VM), and to 600 °C in air for 4 h to obtain ash amount. Then, the fixed carbon (FC) that remains after drying and devolatilization was calculated by subtracting the percentage of moisture, volatile matter, and ash from 100 %.

The gasifier, the cleaning system, the inlet and outlet of the internal combustion engine and the heat exchangers were equipped with temperature, pressure and flow measurement devices. 12 thermocouples type K with isolated hot junction for high temperature (800 °C) were used to monitor the temperature inside the ECO20X system. The accuracy in the range 0 °C–1000 °C was  $\pm(0.4 \%$  reading value) [16]. Ten pressure transducers were employed for measuring the pressure in the hydraulic circuits of the system and a Pitot tube was used for measuring the flow rate of the exhausts leaving the ICE.

## 4. Discussion of results

### 4.1. Energy results

Table 2 reports the data obtained by experimental measurements employed for carrying out the energy and exergy balances. The biomass flow rates entering the ECO20X are obtained by measuring the total mass entering the gasifier through the hopper and dividing it by the time interval. The briquette mass flow rate is about 35 % greater than the one for the pine wood chips. It can also be seen that the electric power using pine wood chips is larger than using briquette, 19.95 kW<sub>e</sub> and 18.17 kW<sub>e</sub>, respectively. These values are averaged over a time interval. The reduction of about 9 % on electric power cannot be motivated only when comparing the LHV of the two biomasses, since the percentage reduction

**Table 3**  
Composition of the biomass (*ar*) and syngas.

Biomass composition ( <i>ar</i> )				
	Pine wood chips		Briquette	
	[w/w %]		[w/w %]	
<i>C</i>	37.20		39.40	
<i>H</i>	4.40		4.73	
<i>N</i>	0.20		1.37	
<i>O</i>	42.00		34.90	
<i>Ash</i>	0.3		11.10	
<i>Moisture</i>	15.90		8.50	
Syngas composition				
	[v/v %]	[w/w %]	[v/v %]	[w/w %]
<i>H<sub>2</sub></i>	18.53	1.48	15.82	1.24
<i>N<sub>2</sub></i>	49.08	55.03	55.27	60.73
<i>CO</i>	18.41	20.64	17.56	19.29
<i>CH<sub>4</sub></i>	1.59	1.02	0.76	0.48
<i>CO<sub>2</sub></i>	12.39	21.83	10.58	18.26

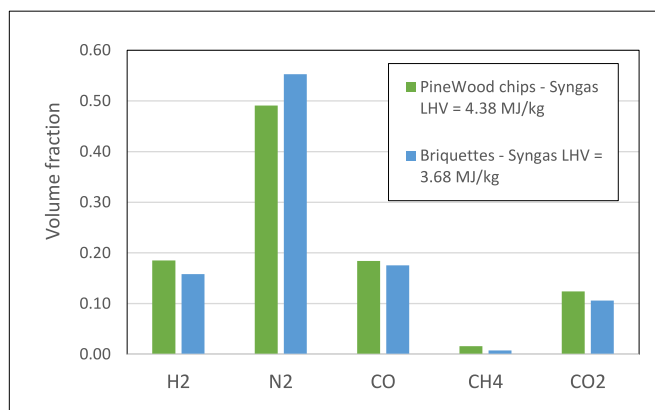


**Fig. 3.** Syngas composition for two biomass substrates and the corresponding LHV values.

is about 14 %.

Table 3 reports the measured elemental composition of the biomass (*ar*), the syngas after the filter section and the exhaust gases from the ICE. These data are required for the computation of energy and exergy balances.

Pine wood chips exhibit a moisture content of 15.9 %, higher than the 8.5 % of briquettes, leading to reduced Lower Heating Value (LHV). However, their low ash content (0.3 %) minimizes operational challenges, in contrast to briquettes, which contain 11.1 % ash. The high ash content in briquettes hinders the efficiency of feedstock conversion into syngas compared to pine wood chips. These values are translated in terms of LHV. In fact, the pine wood chips show an LHV(*ar*) of 12.5 MJ/kg and a corresponding value on a dry basis of 14.8 MJ/kg, whereas for the briquette, the values are 14.2 MJ/kg and 15.5 MJ/kg for *ar* and *dry* basis, respectively.

As far as the syngas composition at the gasifier exit, Fig. 3, it can be observed that the pinewood chip has a larger percentage of H<sub>2</sub>, CO and CH<sub>4</sub>, even if the differences are small. The most important difference is in terms of H<sub>2</sub> volume percentage together with a larger N<sub>2</sub> fraction for the briquette, which accounts for a reduction of about 16 % of the LHV syngas produced by the briquette compared with the pinewood chip [22]. The composition of the syngas affects the LHV, which is 4.38 MJ/kg for the pinewood chips and 3.68 MJ/kg for the briquette. This indicates that gasification is more effective when using pinewood chips rather than briquettes, primarily due to the lower ash content in the former [7,35]. This is confirmed when the efficiency indices are displayed in the next. Furthermore, syngas derived from pine wood chips exhibited higher hydrogen (18.53 %) and carbon monoxide (18.41 %) concentrations, enhancing combustion efficiency and resulting in a higher electrical output of 19.95 kW<sub>e</sub> compared to 18.17 kW<sub>e</sub> for briquettes. While briquettes offer advantages in terms of lower moisture content (8.5 % vs. 15.9 % for pine wood chips), this is outweighed by their higher ash content, which impacts both gasification efficiency and long-term operational stability. These differences underscore the suitability of pine wood chips for applications requiring high efficiency and reliability, whereas briquettes may be more appropriate where feedstock cost is a primary concern.

Using the collected data from experimental tests, the energy balance results are reported in Fig. 4 using the Sankey diagram. Since the biomass flow rates are different, the results are displayed in terms of specific energy (MJ/kg), based on the biomass flow rate. It can be observed that for the specific experimental tests carried out, the energy flows give evidence of the main results of the experimental tests using the two biomass feedstocks. The useful energies are electric and thermal, and the specific values are different for the two feedstocks. The pine-wood chips show a power of 2.50 MJ/kg and a total heat recovery of 3.36 MJ/kg. The briquettes display values of 1.69 and 2.81 MJ/kg,

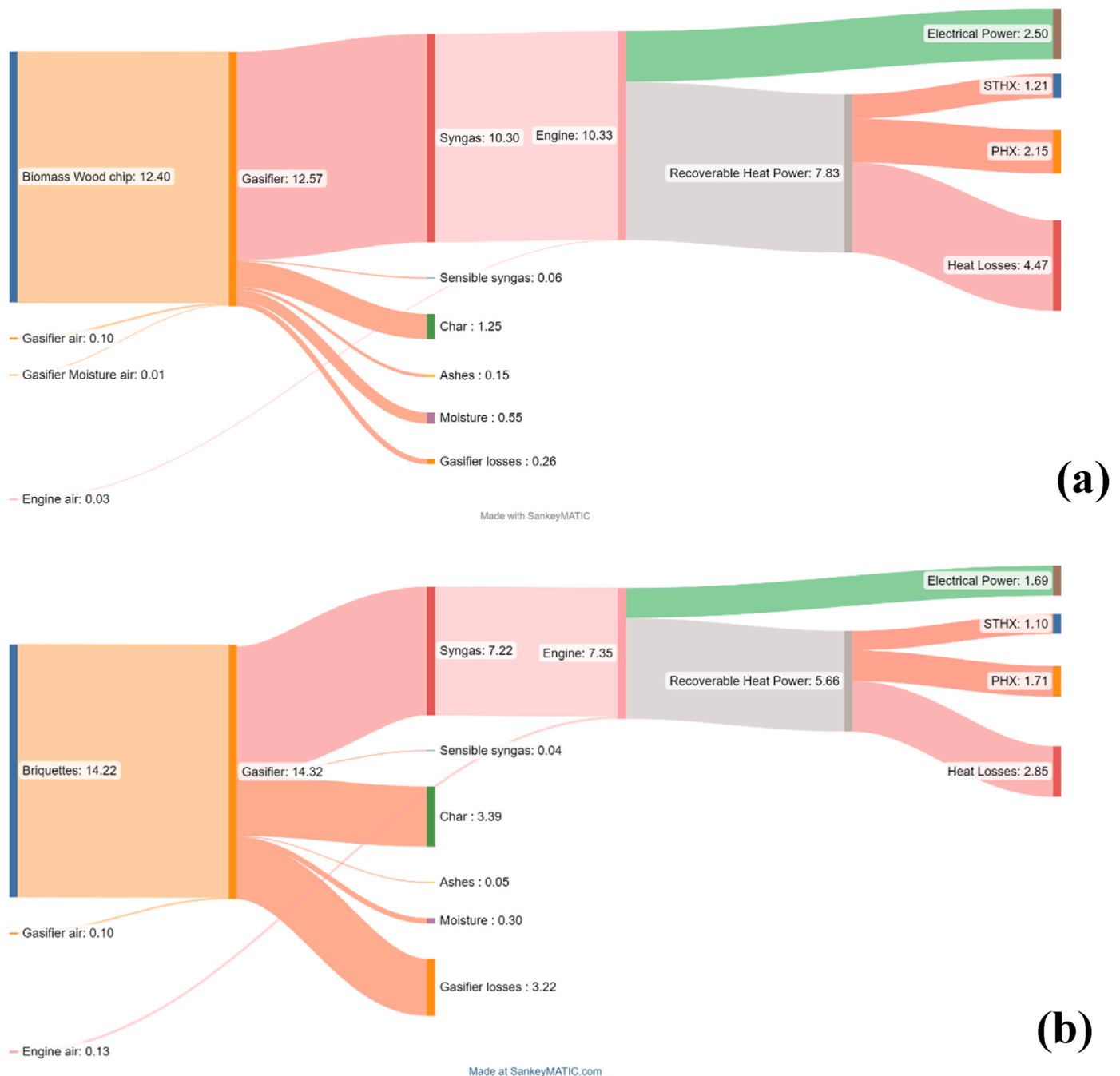


Fig. 4. Sankey diagrams for the two biomasses. All data are expressed in MJ/kg: (a) Pine Wood chips; (b) Briquettes.

**Table 4**  
Efficiencies of the ICE and plant for the two investigate biomasses (in parenthesis nominal efficiencies).

Quantity	Pinewood chips [%]	Briquettes [%]
CGE	82.8	51.0
$\eta_{el,ICE}$	24.3	23.4
$\eta_{th,ICE}$	32.5 (48.7)	39.0 (45.5)
$\eta_{gl,ICE}$	56.8 (72.9)	62.4 (68.8)
$\eta_{gl,pl}$	47.0 (60.4)	31.7 (34.9)

respectively. Using these data, efficiencies of the plant can be obtained comparing the two employed feedstocks, and they are reported in Table 4. The CGE is largely smaller when considering the briquettes because the gasification process is not very efficient using this feedstock, with a value of 51 %, compared to around 83 % for the pinewood chips, most probably because of the high ash content. Pressure and temperature inside the gasifier were analyzed during the tests and two important aspects emerged in the evaluation of the efficiency of the gasification process. During briquetting test, in fact, the average temperature measured in the oxidation zone was significantly higher (915 °C vs 851 °C measured during woodchip test), indicating a greater Equivalence Ratio, as measured and equal to 0.22 for the pine wood chips and 0.25 for the briquettes. This higher ER value negatively influenced the syngas composition, with an increase in N<sub>2</sub> and a decrease in CH<sub>4</sub> content.

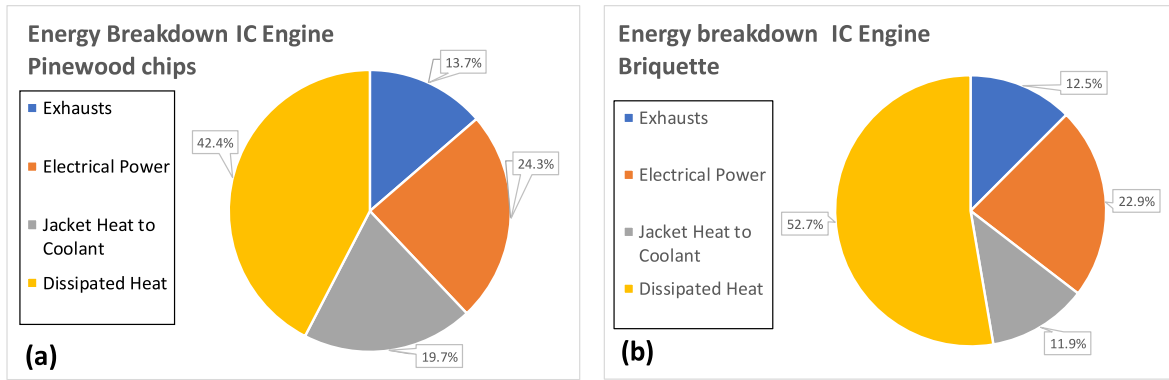


Fig. 5. Energy breakdown in ICE: (a) Pinwood chips; (b) Briquettes.

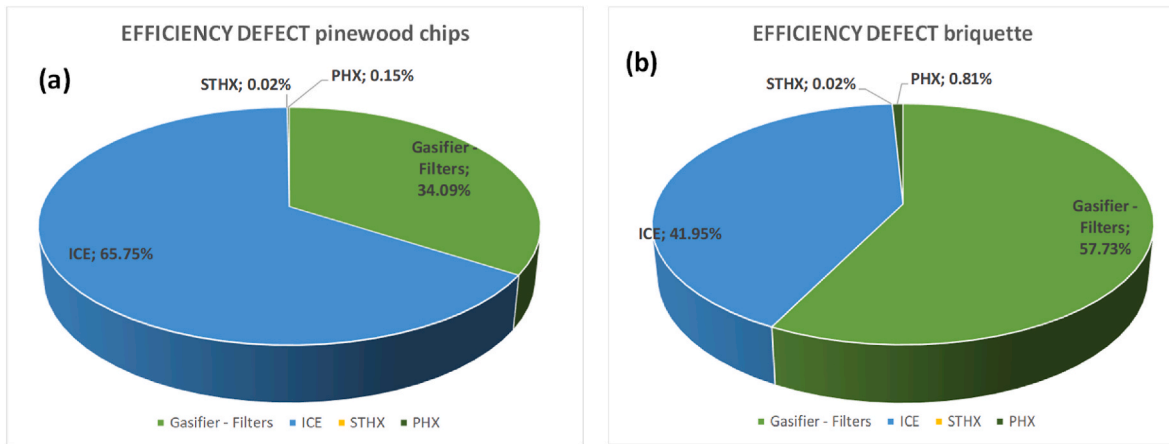


Fig. 6. Exergy defects: a) Pinwood chips; b) Briquettes.

**Table 5**  
Exergy efficiency of the gasifier, ICE and plant.

Quantity	Pine Wood chips [%]	Briquettes [%]
$\eta_{ex,g}$	71.8	49.0
$\eta_{ex,ICE}$	28.9	28.6
$\eta_{ex,pl}$	20.8	14.0

Moreover, the pressure drops inside the reactor doubled during the briquette’s test, from 21 mbar to 41 mbar, indicating a probable accumulation of ashes in the bottom of the reactor. The superior quality of syngas derived from pine wood chips enhances the engine’s energy and exergy efficiencies. This results in an electrical efficiency of 24.3 % for pine wood chips compared to 23.4 % for briquettes. The ash content in briquettes contributes to operational challenges, such as increased pressure drops in the gasifier and potential clogging, further reducing efficiency. Thermal efficiency is influenced by the user’s capacity to utilize the maximum (nominal) thermal power, which was not always fully absorbed during the tests. Consequently, the heat delivered to the user resulted in efficiency values of 32.5 % and 39 % for pine wood chips and briquettes, respectively. Anyway, the nominal thermal efficiency values, reported in parenthesis and italic in Table 4, account for 48.7 and 45.5 %. The global efficiency values obtained from the current tests are 56.8 and 47.0 % for the ICE and plant efficiencies considering the pinewood chips, whereas they are 62.4 and 31.7 % for the briquettes. If the nominal thermal capacity of the plant is considered, the efficiencies would be: 72.9 and 60.4 % for the pinewood chips and 68.8 and 34.9 for the briquettes. The ICE has been designed with a cogeneration ratio  $\gamma = 0.5$ .

The percent energy breakdown at the exit of the energy flow of the ICE is reported in Fig. 5. It can be observed that the qualitative energy breakdown is quite similar, with the largest part represented by the dissipated heat. Quantitatively, the ICE fueled with the two syngas display different values. The electrical power is 24.3 % for Pinewood chips and 22.9 % for the briquettes. The jacket heat to coolant, which represents the possible thermal recovery is about 20 % for the chips and 12 % for the briquettes. The power streamed away by the exhausts accounts for about 13 % of the total energy breakdown in both cases.

4.2. Exergy results

It is evident that feeding the plant with pinewood chips is more efficient than using the briquettes. In fact, as already shown in terms of

**Table 6**  
Economic main parameters employed for the calculation.

Scenario	WACC [%]	P <sub>b</sub> m [€/ton]	P <sub>ee</sub> [€/kWh]	P <sub>CNG</sub> [€/Smc]	H <sub>eq</sub> [h/y]
A1	5.0	0	0.28	1.0	3500
B1	5.0	70	0.28	1.0	3500
C1	5.0	0	0.56	1.25	3500
D1	5.0	70	0.56	1.25	3500
A2	7.50	0	0.28	1.0	3500
B2	7.50	70	0.28	1.0	3500
C2	7.50	0	0.56	1.25	3500
D2	7.50	70	0.56	1.25	3500
A3	7.50	0	0.28	1.0	5000
B3	7.50	70	0.28	1.0	5000
C3	7.50	0	0.56	1.25	5000
D3	7.50	70	0.56	1.25	5000

**Table 7**  
Main Economic indicator results for different scenarios.

Scenario	NPV [€]	PI [%]	SPB [y]	DPB [y]
A1	72,491	32%	7.53	9.68
A2	29,419	13%	7.53	11.49
A3	156,970	68%	5.05	6.57
B1	-264	0%	9.91	14.02
B2	-32,977	-14%	9.91	18.80
B3	67,834	29%	6.56	9.36
C1	307,358	134%	4.24	4.88
C2	230,842	100%	4.24	5.29
C3	444,718	193%	2.89	3.38
D1	234,603	102%	4.90	5.76
D2	168,447	73%	4.90	6.33
D3	355,582	155%	3.33	3.98

energy efficiencies, the pinewood chips perform better than the briquettes. As far as the exergy results, the efficiency defects of the plant fed with the two different biomass feedstocks are displayed in Fig. 6. The larger irreversibility for the pinewood chips is located in the ICE with about 65 % and the gasifier accounts only for 34 % of the total irreversibility in the plant. The situation is reversed when the briquettes are considered. In this case the largest irreversibility is in the gasifier-filters group with around 58 % of the total value.

The exergy efficiencies are reported in Table 5. It is evident that the largest difference between the two feedstocks is in the gasifier, with the pinewood chips which account for 71.8 % exergy efficiency and only 49.0 % for the briquettes. The exergy efficiency of the plant is deeply affected by the gasifier exergy efficiency since the exergy efficiency of the ICE are quite similar for the two feedstocks. Such a low value of the exergy efficiency of the gasifier, 49 %, brings the plant efficiency to 14 %.

4.3. Economic results

Different scenarios have been investigated in the economic analysis. The parameters employed for computing the economic results for different scenarios are the WACC, the cost of electricity and the cost of natural gas bought for energy purposes, the possible availability in situ of the biomass (free or purchasing for it) and the equivalent hours,  $H_{eq}$ , of the cogeneration plant, set equal to 3500 or 5000 h/y. Several hypotheses were employed to compute the economic impact of the micro cogeneration plant with gasifier, among the others the lifetime of the project set equal to 15 years, electrical and thermal energies from the cogeneration plant completely delivered to the users, so no wastefulness of energy is accounted for in the computation.

When not available on the site, the purchase price of the

**Table 8**  
 $CO_{2eq}$  (t/y) savings of ECO20X using the two feedstocks.

	Pine Wood Chips		Briquettes	
$H_{eq}$ (h/y)	3500	5000	3500	5000
Electric Energy (kWh <sub>e</sub> /y)	69825	99750	63595	90850
Thermal Energy (kWh <sub>th</sub> /y)	139650	199500	127190	181700
Saved $CO_{2,eq}$ EE (t/y)	37.74	53.91	34.37	49.10
Saved $CO_{2,eq}$ TH (t/y)	28.45	40.64	25.91	37.01
<b>Total <math>CO_{2eq}</math> saved (t/y)</b>	<b>66.19</b>	<b>94.55</b>	<b>60.28</b>	<b>86.12</b>

lignocellulosic biomass, specifically pine wood,  $p_{bm}$ , has been assumed equal to 70 €/ton. The purchase costs of electric energy and CNG, including taxes, have been chosen considering two different situations: one scenario identified as cheap,  $p_{ee} = 28.0$  €/MWh and  $p_{CNG} = 1.00$  €/Smc, and the other, the expensive one, with  $p_{ee} = 56.0$  €/MWh and  $p_{CNG} = 1.25$  €/Smc.

The whole set of economic parameters produced several scenarios which have been investigated and reported in Table 6.

The calculations accomplished evidence that the economic indicators are largely positive for most of the investigated scenarios, Table 7, showing large savings and thus economic convenience. Table 7 is reported as a heat map to give an immediate visual impact of the best and worst scenarios found in the computations. The red cells indicate the worst case whereas in green the best ones and those in yellow a neutral situation, in which there is an economic convenience on buying the mCHP system. The most unfavorable scenario gives a negative NPV and a DPB which is beyond the lifetime of the project; this is case B2, with the lowest energy purchase costs from the grid and the need to buy the biomass. In addition, the lowest  $H_{eq}$  value means that smaller quantities of energy are delivered by the mCHP system to the user. On the opposite side, when the purchase costs of energies from the grid are higher and the biomass is freely available, in this case the best economic performance of the system is obtained. In detail, scenario C3 gives a NPV value of about 445,000 € with a DPB less than four years and a PI of around 200 %. Considering a similar case, with the cost of purchased energies at low levels, the situation is still worth of attention, because the PI is about 70 % with a DPB of 6.6 years. Except for two scenarios, B1 and B2, in any case there is an interesting saving of money when using the m-CHP, with short and interesting DPB, with the worst case a DPB equal to 11.5 years and the best situation equal to 3.4 years.

4.4.  $CO_{2eq}$  emission reduction analysis

The evaluation of  $CO_{2eq}$  savings was conducted using data from Ref. [36]. Low-voltage electricity generation is associated with emissions of 540.4  $g_{CO_{2eq}}/kWh_e$ , while natural gas boilers emit approximately 203.7  $g_{CO_{2eq}}/kWh_{th}$ . Assuming biomass combustion is carbon-neutral, the resulting  $CO_{2eq}$  savings (t/y) using the ECO20X mCHP system, calculated for the two biomass feedstocks, are presented for annual equivalent operating hours,  $H_{eq}$ , of 3500 and 5000 h in Table 8. The calculations account for the differing yearly electric and thermal energy outputs generated by the two feedstocks. These variations are due to differences in their chemical and physical properties. The cogeneration ratio of 0.5 is assumed.

For electric energy savings, pine wood chips achieve 69,825 kWh annually at 3500 h of operation and 99,750 kWh at 5000 h, whereas briquettes reach 63,595 kWh and 90,850 kWh, respectively. Thermal energy savings follow a similar pattern, with pine wood chips delivering 139,650 kWh annually at 3500 h and 199,500 kWh at 5000 h, compared to briquettes' 127,190 kWh and 181,700 kWh. These differences underline the superior efficiency of pine wood chips, likely due to their higher quality syngas output and lower ash content, which enhance gasification performance.

The  $CO_{2eq}$  savings reflect these energy differences. For electricity, pine wood chips save 37.74 tons annually at 3500 h and 53.91 tons at 5000 h, compared to 34.37 tons and 49.10 tons for briquettes. Similarly, for thermal energy, pine wood chips result in 28.45 tons of  $CO_{2,eq}$  savings annually at 3500 h and 40.64 tons at 5000 h, while briquettes save 25.91 tons and 37.01 tons, respectively. Overall, the total  $CO_{2,eq}$  savings demonstrate the environmental advantages of these systems. Pine wood chips provide total annual savings of 66.19 tons at 3500 h and 94.55 tons at 5000 h, while briquettes offer 60.28 tons and 86.12 tons under the same conditions. These results highlight the significant potential of biomass CHP systems for reducing emissions, with pine wood chips showing a clear advantage in terms of both efficiency and environmental impact. Longer operational hours further enhance these benefits,

making such systems an effective solution for sustainable energy generation.

## 5. Conclusions

An energy, exergy and economic analysis of a micro-cogeneration system coupled with a wood biomass downdraft gasifier has been accomplished. Two types of different biomass feedstocks have been tested: Briquette from pruning and Pine wood chips. The electrical power of the combined system was obtained and compared, and the efficiency of the whole system was evaluated. Woodchip shows greater efficiency and energy yield, but it could be a cost to add in terms of supply. Conversely, briquettes from pruning waste and maintenance of green areas, although less efficient, are an excellent way to energetically and economically enhance a material that would otherwise be disposed of as waste. The efficiency indexes are larger for pinewood chips than for briquettes, mainly because the efficiency of the gasifier for briquettes is much lower than for pinewood chips. In fact, the CGE is around 83 % for pinewood chips and 49 % for briquettes. Global efficiency accounts for 47 % versus 31 %, with the efficiency indices of the sole cogeneration plant quite similar, around 60 % for the experimental tests carried out. The economic indexes are very favorable, with a Profitability Index ranging between 32 % and 193 % when positive, assuming a lifetime of the plant equal to 15 years, and very interesting Discounted Payback times, between 3.4 and 11.5 years. In scenarios where grid energy prices are high, the savings increase dramatically. For example, in the most favorable scenario (free biomass and high energy prices from the grid), the system achieves a Net Present Value (NPV) of €445,000 over a 15-year lifetime. The system offers up to a 70 % reduction in energy costs compared to traditional solutions reliant on natural gas or grid electricity. Even in less favorable cases (e.g., purchased biomass and low grid energy prices), the system still demonstrates financial viability with payback times under 12 years.

The total CO<sub>2eq</sub> savings highlight the significant environmental benefits of biomass CHP systems. Pine wood chips can achieve annual savings of approximately 66 tons at 3500 equivalent hours and around 95 tons at 5000 h. In comparison, briquettes provide savings of 60 tons at 3500 h and 86 tons at 5000 h under the same conditions. These findings emphasize the crucial role that biomass CHP systems play in reducing greenhouse gas emissions and promoting sustainable energy solutions.

Future work will focus on optimizing the gasifier design to handle diverse biomass feedstocks, particularly those with high ash content or variable moisture levels, through structural modifications and improved heat distribution. Enhancing the syngas cleaning system with advanced filtration technologies will improve syngas quality, reduce engine wear, and boost efficiency. Additionally, the use of durable, corrosion-resistant materials will address issues such as high-temperature corrosion caused by alkali metals in biomass feedstocks. A comprehensive life cycle assessment (LCA) will also be conducted to evaluate the system's environmental impact, sustainability, and potential areas for improvement.

## CRedit authorship contribution statement

**B. Morrone:** Writing – original draft, Funding acquisition, Formal analysis, Conceptualization. **P. Bracciano:** Writing – review & editing, Visualization, Software, Investigation. **D. Cirillo:** Writing – review & editing, Writing – original draft, Investigation, Formal analysis, Data curation. **M. La Villetta:** Writing – review & editing, Investigation, Formal analysis. **C. Caputo:** Writing – review & editing, Writing – original draft, Methodology, Formal analysis, Data curation.

## Funding Statement

The research has been partially supported by Italian Ministry of

Environment and Energy Security (formerly of Ecological Transition) in the NEXT GENERATION EU framework (PNRR), “Green revolution and ecological transition”, component 2 “Renewable Energy, Hydrogen, Grid and Sustainable Mobility” under the grant CUP: F29J22001310004 project “SOSPURI”.

## Declaration of competing interest

The authors declare that they have no known competing financial interests or personal relationships that could have appeared to influence the work reported in this paper.

## References

- [1] H. Ritchie, P. Rosado, M. Roser, Emissions by sector: where do greenhouse gases come from? OurWorldInDataOrg (2020). <https://ourworldindata.org/emissions-by-sector>. (Accessed 8 January 2024).
- [2] United Nations, For a livable climate: Net-zero commitments must be backed by credible action (2022). <https://www.un.org/en/climatechange/net-zero-coalition>.
- [3] International Energy Agency, Net Zero by 2050: A Roadmap for the Global Energy Sector (2021).
- [4] Eurostat, Inflation in the Euro area. Inflation in the Euro Area 2023, Eurostat Reports, 2023. [https://ec.europa.eu/eurostat/statistics-explained/index.php?title=Inflation\\_in\\_the\\_euro\\_area#Euro\\_area\\_annual\\_inflation\\_rate\\_and\\_its\\_main\\_components](https://ec.europa.eu/eurostat/statistics-explained/index.php?title=Inflation_in_the_euro_area#Euro_area_annual_inflation_rate_and_its_main_components).
- [5] EU Commission, A European Green Deal Striving to be the first climate-neutral continent 2019 (2018). [https://commission.europa.eu/strategy-and-policy/priorities-2019-2024/european-green-deal\\_en](https://commission.europa.eu/strategy-and-policy/priorities-2019-2024/european-green-deal_en). (Accessed 8 January 2024).
- [6] S. Verma, A.M. Dregulo, V. Kumar, P.C. Bhargava, N. Khan, A. Singh, et al., Reaction engineering during biomass gasification and conversion to energy, Energy 266 (2023), <https://doi.org/10.1016/j.energy.2022.126458>.
- [7] M. Puglia, N. Morselli, F. Ottani, S. Pedrazzi, P. Tartarini, G. Allesina, A preliminary evaluation of different residual biomass potential for energy conversion in a micro-scale downdraft gasifier, Sustain. Energy Technol. Assessments 57 (2023), <https://doi.org/10.1016/j.seta.2023.103224>.
- [8] S. Martinez, G. Michaux, P. Salagnac, J.L. Bouvier, Micro-combined heat and power systems (micro-CHP) based on renewable energy sources, Energy Convers. Manag. 154 (2017) 262–285, <https://doi.org/10.1016/j.enconman.2017.10.035>.
- [9] J. Ahrenfeldt, T.P. Thomsen, U. Henriksen, L.R. Clausen, Biomass gasification cogeneration - a review of state of the art technology and near future perspectives, Appl. Therm. Eng. 50 (2013) 1407–1417, <https://doi.org/10.1016/j.applthermaleng.2011.12.040>.
- [10] D. Perrone, T. Castiglione, P. Morrone, F. Pantano, S. Bova, Numerical and experimental assessment of a micro-combined cooling, heating, and power (CCHP) system based on biomass gasification, Appl. Therm. Eng. 219 (2023), <https://doi.org/10.1016/j.applthermaleng.2022.119600>.
- [11] A. Galvagno, M. Prestipino, V. Chiodo, S. Maisano, S. Brusca, R. Lanzafame, Biomass blend effect on energy production in a co-gasification-CHP system, AIP Conf. Proc. 2191 (2019), <https://doi.org/10.1063/1.5138815>. American Institute of Physics Inc.
- [12] C.T. Chang, M. Costa, M. La Villetta, A. Macaluso, D. Piazzullo, L. Vanoli, Thermo-economic analyses of a Taiwanese combined CHP system fuelled with syngas from rice husk gasification, Energy 167 (2019) 766–780, <https://doi.org/10.1016/j.energy.2018.11.012>.
- [13] P. Jie, Z. Li, Y. Ren, F. Wei, Economy-energy-environment optimization of biomass gasification CCHP system integrated with ground source heat pump, Energy 277 (2023), <https://doi.org/10.1016/j.energy.2023.127554>.
- [14] P. Klimantos, N. Koukouzas, A. Katsiadakis, E. Kakaras, Air-blown biomass gasification combined cycles (BGCC): system analysis and economic assessment, Energy 34 (2009) 708–714, <https://doi.org/10.1016/j.energy.2008.04.009>.
- [15] U. Arena, F. Di Gregorio, M. Santonastasi, A techno-economic comparison between two design configurations for a small scale, biomass-to-energy gasification based system, Chem. Eng. J. 162 (2010) 580–590, <https://doi.org/10.1016/j.cej.2010.05.067>.
- [16] M. La Villetta, M. Costa, D. Cirillo, N. Massarotti, L. Vanoli, Performance analysis of a biomass powered micro-cogeneration system based on gasification and syngas conversion in a reciprocating engine, Energy Convers. Manag. 175 (2018) 33–48, <https://doi.org/10.1016/j.enconman.2018.08.017>.
- [17] M. Costa, V. Rocco, C. Caputo, D. Cirillo, G. Di Blasio, M. La Villetta, et al., Model based optimization of the control strategy of a gasifier coupled with a spark ignition engine in a biomass powered cogeneration system, Appl. Therm. Eng. 160 (2019) 114083, <https://doi.org/10.1016/j.applthermaleng.2019.114083>.
- [18] European Union, Shedding light on energy in Europe - 2024 edition. <https://ec.europa.eu/eurostat/web/interactive-publications/energy-2024#about-publication>, 2024. (Accessed 21 April 2024).
- [19] V.R. Patel, D. Patel, N.S. Varia, R.N. Patel, Co-gasification of lignite and waste wood in a pilot-scale (10 kW) downdraft gasifier, Energy 119 (2017) 834–844, <https://doi.org/10.1016/j.energy.2016.11.057>.
- [20] M. Puglia, N. Morselli, F. Ottani, S. Pedrazzi, P. Tartarini, G. Allesina, A preliminary evaluation of different residual biomass potential for energy conversion in a micro-scale downdraft gasifier, SSRN Electron. J. 57 (2022), <https://doi.org/10.2139/ssrn.4163794>.

- [21] K. Mishra, S. Singh Siwal, A. Kumar Saini, V.K. Thakur, Recent update on gasification and pyrolysis processes of lignocellulosic and algal biomass for hydrogen production, *Fuel* 332 (2023) 126169, <https://doi.org/10.1016/j.fuel.2022.126169>.
- [22] P.R. Havilah, A.K. Sharma, G. Govindasamy, L. Matsakas, A. Patel, Biomass gasification in downdraft gasifiers: a technical review on production, up-Gradation and application of Synthesis gas, *Energies* 15 (2022), <https://doi.org/10.3390/en15113938>.
- [23] P.K. Ghodke, A.K. Sharma, A. Jayaseelan, K.P. Gopinath, Hydrogen-rich syngas production from the lignocellulosic biomass by catalytic gasification: a state of art review on advance technologies, economic challenges, and future prospectus, *Fuel* 342 (2023), <https://doi.org/10.1016/j.fuel.2023.127800>.
- [24] Z. Xiao, W. Wu, Environmental sustainability by an integrated system based on municipal solid waste fluidized bed gasification using energy, exergy, and environmental analyses, *Appl. Therm. Eng.* 239 (2024), <https://doi.org/10.1016/j.applthermaleng.2023.122171>.
- [25] B. Ojha, M. Schober, S. Turad, J. Jochum, H. Kohler, Gasification of biomass: the very sensitive monitoring of tar in syngas by the Determination of the oxygen demand—a Proof of Concept, *Processes* 10 (2022), <https://doi.org/10.3390/pr10071270>.
- [26] J. Cai, Y. He, X. Yu, S.W. Banks, Y. Yang, X. Zhang, et al., Review of physicochemical properties and analytical characterization of lignocellulosic biomass, *Renew. Sustain. Energy Rev.* 76 (2017) 309–322, <https://doi.org/10.1016/j.rser.2017.03.072>.
- [27] S.M. Chern, W.P. Walawender, L.T. Fan, *Mass and Energy Balance Analyses of a Downdraft Gasifier*, vol. 18, 1989.
- [28] S.A. Channiwala, P.P. Parikh, A unified correlation for estimating HHV of solid, liquid and gaseous fuels, *Fuel* 81 (2002) 1051–1063, [https://doi.org/10.1016/S0016-2361\(01\)00131-4](https://doi.org/10.1016/S0016-2361(01)00131-4).
- [29] C. Sheng, J.L.T. Azevedo, Estimating the higher heating value of biomass fuels from basic analysis data, *Biomass Bioenergy* 28 (2005) 499–507, <https://doi.org/10.1016/j.biombioe.2004.11.008>.
- [30] M. Costa, V. Rocco, C. Caputo, D. Cirillo, G. Di Blasio, M. La Villetta, et al., Model based optimization of the control strategy of a gasifier coupled with a spark ignition engine in a biomass powered cogeneration system, *Appl. Therm. Eng.* 160 (2019), <https://doi.org/10.1016/j.applthermaleng.2019.114083>.
- [31] T.J. Kotas, *The Exergy Method of Thermal Plant Analysis*, Elsevier, 1985, <https://doi.org/10.1016/C2013-0-00894-8>.
- [32] G. Towler, R. Sinnott, *CHEMICAL ENGINEERING DESIGN Principles, Practice and Economics of Plant and Process Design*, Butterworth-Heinemann, 2008.
- [33] M. Peters, K. Timmerhaus, R. West, *Plant Design and Economics for Chemical Engineers*, fifth ed., McGraw-Hill Higher Ed, New York, 2002.
- [34] P. Basu, P. Kaushal, Biomass gasification, pyrolysis and Torrefaction, in: P. Basu, P. Kaushal (Eds.), *Biomass Gasification, Pyrolysis, and Torrefaction*, fourth ed., Academic Press, 2024, p. v, <https://doi.org/10.1016/B978-0-443-13784-6.00030-5>.
- [35] K. Mishra, S. Singh Siwal, A. Kumar Saini, V.K. Thakur, Recent update on gasification and pyrolysis processes of lignocellulosic and algal biomass for hydrogen production, *Fuel* 332 (2023), <https://doi.org/10.1016/j.fuel.2022.126169>.
- [36] J. Giuntoli, A. Agostini, R. Edwards, L. Marelli, Solid and gaseous bioenergy pathways: input values and GHG emissions. Calculated according to the methodology set in COM (2016), <https://doi.org/10.2790/27486>, 767 EUR 27215 EN. 2017.